

## Synchrony suppression in ensembles of coupled oscillators via adaptive vanishing feedback

Ghazal Montaseri<sup>1,2</sup>, Mohammad Javad Yazdanpanah<sup>3</sup>, Arkady Pikovsky<sup>2</sup>, and Michael Rosenblum<sup>21</sup>

<sup>1</sup>*Advanced Control Systems Laboratory, School of Electrical and Computer Engineering, College of Engineering, University of Tehran, Tehran, Iran*

<sup>2</sup>*Department of Physics and Astronomy, University of Potsdam, Karl-Liebknecht-Str. 24/25, 14476 Potsdam, Germany*

<sup>3</sup>*Advanced Control Systems Laboratory, Control and Intelligent Processing Center of Excellence, School of Electrical and Computer Engineering, College of Engineering, University of Tehran, Tehran, Iran*

(Dated: 8 September 2021)

Synchronization and emergence of a collective mode is a general phenomenon, frequently observed in ensembles of coupled self-sustained oscillators of various natures. In several circumstances, in particular in cases of neurological pathologies, this state of the active medium is undesirable. Destruction of this state by a specially designed stimulation is a challenge of high clinical relevance. Typically, the precise effect of an external action on the ensemble is unknown, since the microscopic description of the oscillators and their interactions are not available. We show, that desynchronization in case of a large degree of uncertainty about important features of the system is nevertheless possible; it can be achieved by virtue of a feedback loop with an additional adaptation of parameters. The adaptation also ensures desynchronization of ensembles with non-stationary, time-varying parameters. We perform the stability analysis of the feedback-controlled system and demonstrate efficient destruction of synchrony for several models, including those of spiking and bursting neurons.

PACS numbers: 05.45.Xt Synchronization; coupled oscillators

87.19.lr Control theory and feedback

87.19.L- Neuroscience

Synchronization is a general effect in coupled oscillator systems: due to an adjustment of individual rhythms, the objects start to oscillate in tact, producing a pronounced collective rhythm. This is observed not only in physical and technical systems (lasers, Josephson junctions, spin-torque oscillators, metronomes) but in many biological (e.g. fireflies) and even social (applause) systems. Synchronization can be influenced by an external forcing of the system. In some situations synchrony is not desirable: e.g., Parkinson's tremor is attributed to a pathological synchrony in population of neurons in the brain. One tries to suppress this synchrony by a properly designed external forcing, which is arranged via a proportional feedback. In this respect, suppression of synchrony can be treated as a control problem. The main difficulty here is that the particular mechanism, of effects of forcing on oscillating elements is not known. To overcome this problem, we suggest here an adaptive scheme which adjusts the parameters of the feedback loop and, thus, compensates the absence of knowledge about microscopic organization of the ensemble. We demonstrate the feasibility of this approach on several examples, including also highly non-stationary situations where readjustment of the parameters is needed.

---

## I. INTRODUCTION

Synchronization is adjustment of rhythms of coupled oscillating objects due to their weak interaction<sup>1</sup>. In physics, biology, engineering, and neuroscience, a wide range of synchronization phenomena in large oscillator populations is known, such as coordinated firing of cardiac pacemaker cells, synchronous regimes in arrays of Josephson junctions and lasers, synchronization in ensembles of electronic circuits and in neuronal populations<sup>1-4</sup>.

In neuroscience, synchronization of neurons plays an important role in vital functions like vision, movement control, and memory<sup>5</sup>. On the other hand, such diseases as epilepsies, Parkinson's disease, and essential tremor are believed to be related to a pathologically enhanced synchronization of neurons<sup>6-10</sup>. Many patients suffering from these diseases cannot be cured by known medications and are therefore treated by Deep Brain Stimulation (DBS) which implies stimulation of the brain tissue via implanted microelectrodes<sup>11-15</sup>. Typically,

the stimulation is delivered by a subcutaneously implanted controller. In its present form, DBS is a permanent open-loop stimulation with high frequency (about 120 Hz) pulses; in neurological practice the controller's parameters are tuned empirically. DBS is known to cause serious side-effects like speech problems and involuntary muscle contractions. Besides, permanent intervention into the brain tissue results in fast discharge of the controller's batteries, and, consequently, in further minor surgery. Despite DBS clinical success, its exact mechanism is not yet completely understood<sup>16</sup>. Presumably, the effect of high-frequency stimulation is not related to desynchronization of neurons, but rather to lesioning of the tissue via suppression of the neuronal activity.

DBS limitations and high clinical relevance have encouraged experimentalists to search for more efficient stimulation algorithms. So, a feedback-based DBS has been recently tested in a study with primate model of Parkinson's disease<sup>17</sup> and with rodent model of epilepsy<sup>18</sup>. Besides these empirical studies, there were quite a number of theoretical efforts within the physical and engineering community. The key idea of this activity, initiated by P. Tass<sup>6,19</sup>, is that the stimulation should be able to suppress the abnormal synchrony among neurons without putting them to silence, or, in physical terms, to desynchronize the synchronized oscillators without quenching them. In this approach the neuronal population is typically modeled as a network with high connectivity and treated in the mean field approximation. The mean field of the ensemble is associated with the pathological brain rhythm; hence, the goal of the stimulation is to minimize the mean field.

There are two groups of desynchronizing techniques. The first group is based on the idea of phase resetting by precisely timed pulses<sup>6,19,20</sup>, while the second group involves the methods from the control theory and relies on continuous feedback<sup>21,22</sup>. The latter is based on the measurement of the mean field which one wants to diminish. The feedback may be proportional to the mean field or its delayed value, or be a nonlinear function of it<sup>21-32</sup>. Multi-site feedback controllers are considered in<sup>33-35</sup>. Feedback control of two interacting subpopulations is addressed in<sup>29,36,37</sup>. In the context of the neuroscience application, the crucial feature of the feedback schemes is their potential ability to provide *vanishing stimulation control*, i.e. to ensure that the stimulation tends to zero (to be exact, to the noise level), as soon as the goal of the control is achieved and the undesired synchrony is suppressed<sup>22,24</sup>. In the present contribution we extend the results of<sup>24</sup>, designing an adaptive vanishing stimulation setup.

In many applications, in particular in neuroscience, the mechanism of external action on individual oscillators and their interactions is not fully understood. So, when an electric stimulation of the brain tissue is applied via an implanted electrode, many factors regarding the impact of the stimulation remain unknown, e.g., whether the stimulation affects only the membrane voltage of a cell or it may influence the gating variables; next, it is not exactly known how the effect of stimulation decreases with the distance from the electrode or how its impact changes with time, etc. Thus, the feedback control we want to design shall work without good knowledge of the system to be controlled and shall exploit only rather general models of emergent collective activity. It means that the controller shall be able to cope with the uncertainty and, possibly, with the time drift of parameters of the system. These considerations motivated us to implement an adaptive control strategy and to modify the stimulation technique proposed in<sup>24</sup> to ensure adaptive vanishing stimulation.

The paper is organized as follows. In Section II we reformulate the problems in terms of the control theory and discuss the required features of the controller. In Section III we discuss the design of the feedback controller and in Section IV we analyze its stability. Section V presents the examples of synchrony suppression in several models of globally coupled oscillators. In Section VI we summarize our results. Some details of the stability analysis and of numerical simulations are given in Appendices.

## II. DESYNCHRONIZATION AS A CONTROL PROBLEM

Consider an ensemble of  $N$  coupled self-sustained oscillators. At the microscopic level, depending on the coupling strength, oscillators may oscillate incoherently (or asynchronously) or they may show (partially) synchronous oscillations. At the macroscopic level, i.e. where only the collective motion of the ensemble is considered, a transition to synchrony can be viewed as a Hopf bifurcation, which is described by the normal form

$$\dot{Z} = (\xi + i\omega_0)Z - |Z|^2 Z, \quad (1)$$

also known as the Stuart-Landau equation. Here  $Z$  and  $\omega_0$  are the complex amplitude and frequency of the collective mode (mean field), respectively, and parameter  $\xi > 0$  describes the instability of the only equilibrium point  $Z = 0$  of Eq. (1). We emphasize that exact derivation of Eq. (1) from the microscopic dynamics is possible only in exceptional cases (cf.

recent papers<sup>38,39</sup>, where Eq. (1) has been derived for the Kuramoto model of sine-coupled phase oscillators). For general self-sustained oscillators and general coupling, and especially for live systems where the models, if known, are very approximate, this is not feasible, and Eq. (1) remains a phenomenological model equation.

At the macroscopic level, onset of synchronous or asynchronous oscillations is related to the instability or stability of the equilibrium point, respectively. In this framework, the *desynchronization problem* means designing a stimulation (control input)  $u$ , such that the *controlled system*

$$\dot{Z} = (\xi + i\omega_0)Z - |Z|^2Z + e^{i\beta}u \quad (2)$$

is stabilized at the origin. The phase shift parameter  $\beta$  in this model equation reflects the uncertainty in the impact of the stimulation on oscillators. In Ref.<sup>22</sup> some of us have shown that  $\beta$  inevitably appears in the normal form equation of the forced globally coupled system; this parameter depends on the organization of the global coupling in the ensemble and on the properties of individual units (cf. Ref.<sup>40</sup> for a similar phase shift in an optical feedback). Therefore, frequently used assumptions that  $\beta = 0$  or  $\beta = \pi$  are not validated by theory and neglect essential feature of the collective dynamics. Throughout this paper, we consider  $\beta$  as an unknown, possibly time-variant, parameter and assume that it may attain all values within  $[0, 2\pi)$ .

From the control theory point of view, uncertainties modeled by multipliers of the control input represent the *unknown control directions problem*. Designing a stabilizing controller for a system with an unknown control direction is more complicated than for other classes of uncertainties. One intuitive reason is that unknown control multipliers may change the negative feedback to the positive one. The solution of this problem is known for several special cases only. For a scalar system, the solution is obtained using the Lyapunov direct method<sup>41</sup> or with the help of the iterative learning technique<sup>42</sup>. For two-dimensional systems, in Ref.<sup>43</sup> the stabilizing controller with unknown direction is designed if the input  $u$  enters one of the equations only. (If our system (2) is re-written in coordinates,  $X = \text{Re}(Z)$ ,  $Y = \text{Im}(Z)$ , the term  $e^{i\beta}u$  generally appears in both equations for  $\dot{X}$  and  $\dot{Y}$ .) This problem is well studied for a class of nonlinear systems which can be written in the strict feedback form (see e.g.<sup>44-46</sup> and the references therein) or in the normal form<sup>47,48</sup>, or if two control inputs  $u_{1,2}$  are allowed<sup>49</sup>, so that factors  $\cos\beta$  and  $\sin\beta$  can be compensated. This brief review of the existing techniques to the unknown control direction problem shows that they

cannot be exploited for our purpose.

In this paper, we propose a feedback stimulation technique for stabilizing the zero equilibrium point of Eq. (2). The main advantage is that it (i) provides the vanishing control, what reduces the intervention into a living tissue and the energy consumption. Next, the controller (ii) stabilizes the system in the presence of the unknown phase shift  $\beta$  and (iii) is able to adapt itself to variations of  $\beta$ . Having in mind possible neuroscience applications, we also ensure that the designed controller has the following properties. It (iv) performs stabilization using the signal which is contaminated by the rhythms produced by neighboring neuronal populations and the measurement noise. It is able (v) to washout constant component in the measurement. Finally, the stimulation (vi) avoids sudden impacts on the neuronal ensemble, which may force neurons to behave far from their natural dynamics, but affects the ensemble gradually and smoothly.

### III. DESIGNING AN ADAPTIVE STIMULATION

To motivate our approach (and for discussion below), we first mention that the simplest way to linearly stabilize the system (2) at  $Z = 0$  would be to choose  $u = -\gamma e^{-i\beta} Z$ , with  $\gamma > \xi$ . However, the control signal shall be real-valued. If we take  $u = \text{Re}(-\gamma e^{-i\beta} Z) = -\gamma(X \cos \beta + Y \sin \beta)$ , the control action will be also stabilizing. However, since  $Y$  is not available and  $\beta$  is unknown, this scheme cannot be implemented.

By constructing the feedback-based stimulation with the mentioned specifications, we assume that the real-valued measurement  $m = \text{Re}(Z) + b + n$  is available. The constant term  $b$  reflects the fact that the equilibrium point of the macroscopic oscillator is non-zero, what frequently occurs in neuronal models, and  $n$  is noise. The controller consists of three blocks, as illustrated in Fig. 1, where dynamic sub-blocks are shown by squares and static sub-blocks by ellipses. The first block is described by the equations:

$$\dot{x}_1 = x_2, \tag{3}$$

$$\dot{x}_2 = m - \omega_0^2 x_1 - \delta x_2, \tag{4}$$

$$\dot{x}_3 = \frac{1}{\mu}(x_2 - x_3), \tag{5}$$

where Eqs. (3) and (4) constitute a second order bandpass filter which ensures accomplishment of the requirements (iv) and (v). The damping factor  $\delta$  determines the width of the

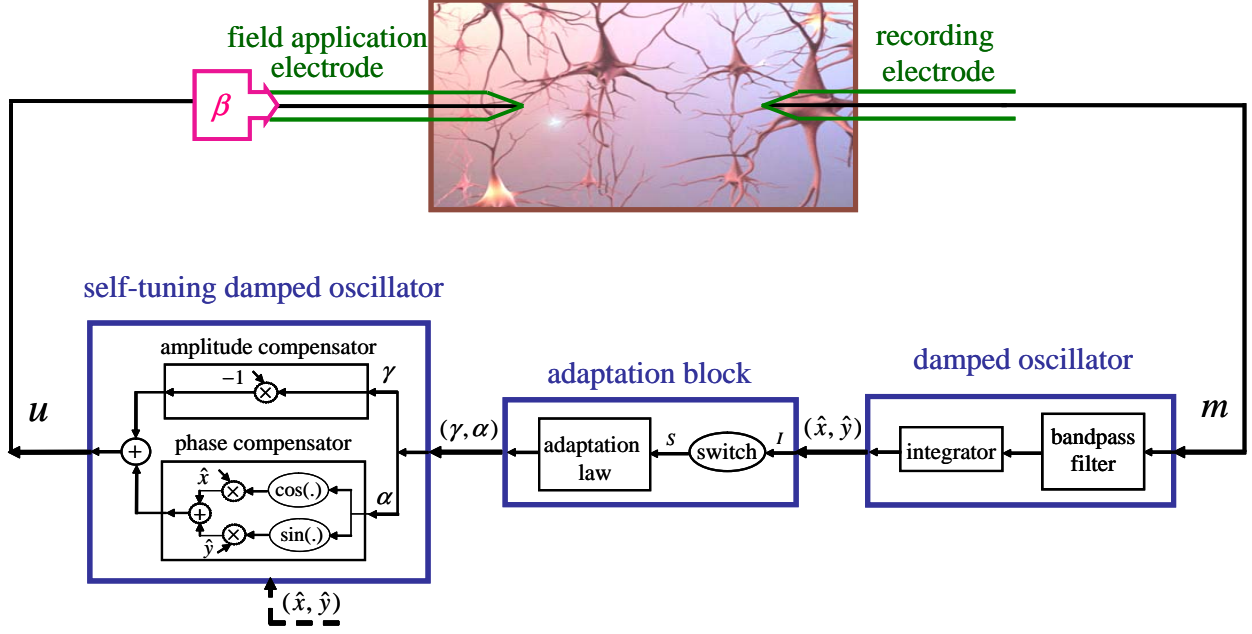


FIG. 1. (Color online) The schematic representation of the controlled neuronal population. The local field potential, related to the mean field of the population, is measured by the recording electrode. The adaptive controller consisting of three blocks generates the control signal which is fed back to the system via the field application electrode. The adaptive nature of the stimulation makes it capable of compensating an *a priori* unknown and slowly varying phase shift parameter  $\beta$ .

bandpass. Frequency  $\omega_0$  is chosen to be close to the basic oscillator frequency of  $Z$ , which can be easily measured in the experiment. Parameter  $\mu$  is chosen so that  $\mu\omega_0 \gg 1$ , then the sub-block (5) operates as an integrator. Thus,  $x_3$  has the same average as  $x_2$  but its phase is shifted by  $\pi/2$ . Finally, we define two *auxiliary oscillating modes* as:

$$\hat{x} = \delta x_2, \quad \hat{y} = \delta \mu \omega_0 x_3. \quad (6)$$

The amplitudes of  $\hat{x}$  and  $\hat{y}$  are close to that of  $m$ , but their phases are shifted by 0 and  $\pi/2$ , respectively.

The second block implements an adaptation mechanism. First, we define an observable  $S$  that is proportional to the oscillation amplitude  $I = \sqrt{\hat{x}^2 + \hat{y}^2}$ , with a cutoff at small amplitudes:

$$S = I [1 + \tanh(k_s(I - h_s))] . \quad (7)$$

Here  $S$  is the positive increasing function of  $I$ ; at the cutoff threshold  $I \approx h_s$  it switches

from exponentially small values to  $S \approx 2I$ , the width of the switching region is governed by  $k_s$ . The cutoff is required due to the following. Although the noise is suppressed in auxiliary oscillating modes  $\hat{x}$  and  $\hat{y}$ , it is not completely canceled. Therefore the cutoff is needed to ignore the noise impact below the threshold value  $I \approx h_s$ . In a population with a finite size  $N$ , the mean field below the synchronization threshold can be treated as a noise with the root mean square (rms) value proportional to  $1/\sqrt{N}$ <sup>50</sup>. So,  $I$  is of the order of  $\sqrt{2/N}$  which estimates the lower bound of  $h_s$ .

In the next block, the transformed signal  $S$  is used to govern the *adaptive variables*  $\alpha$  and  $\gamma$  as:

$$\dot{\alpha} = k_\alpha S, \quad \alpha(0) = 0, \quad (8)$$

$$\dot{\gamma} = k_{\gamma_1} S \cosh^{-1}(k_{\gamma_2} \gamma / \omega_0), \quad \gamma(0) = 0. \quad (9)$$

Here  $k_{\gamma_i}$ ,  $i = 1, 2$  and  $k_\alpha$  are the positive *adaptation parameters*. When the measured signal  $m$  and the auxiliary modes exhibit large oscillations,  $S$  attains some non-zero values. Then,  $\alpha$  and  $\gamma$  start to grow from zero until the desired suppression level is achieved and  $S$  switches off. Due to the inevitable presence of the noise in real applications, if we replace  $S$  with  $I$  in Eqs. (8) and (9), the adaptive variables never settle down, because  $I$  never vanishes exactly. Finally, the term  $\cosh(k_{\gamma_2} \gamma / \omega_0)$  in Eq. (9) is introduced to suppress the undesired increase of  $\gamma$  which may lead to large control effort and large oscillation amplitude in the transient time before the stabilization occurs.

Thus, the first and second blocks generate oscillating modes  $\hat{x}, \hat{y}$  and the adaptive variables  $\alpha, \gamma$ . The final control signal is in fact the oscillating mode, with the phase shifted by  $\alpha$  and the amplitude multiplied by  $\gamma$ :

$$u = -\gamma (\hat{x} \cos \alpha + \hat{y} \sin \alpha). \quad (10)$$

This transformation is accomplished in the last block, consisting of a phase shifting unit and a multiplier.

Now we recall the discussion in the beginning of this Section. We see that the control law Eq. (10) would operate properly if  $\hat{x} \cos \alpha \sim X \cos \beta$  and  $\hat{y} \sin \alpha \sim Y \sin \beta$ . The similarity between these two controllers gives us an intuitive insight about the capability of (10) in stabilizing the zero equilibrium point of the controlled system (quantitative analysis will be presented in the next Section). It is easy to check that the proposed scheme fulfills all above



formulated requirements and provides vanishing control, i.e. the maintenance of the desired asynchronous state needs no control effort.

One important property that makes the proposed adaptive stimulation distinct from other proposed techniques is that the stimulation emerges from the origin (at  $t = 0$ ,  $\gamma = 0$  and thus,  $u = 0$ ), then grows gradually and finally, settles down again at the origin. During its lifetime, it adapts itself until it overcomes the natural coupling between the oscillators and thus leads to desynchronization. Since the stimulation affects the oscillators of the population gradually and smoothly, it avoids undesired sudden impacts on the natural behaviors of the stimulated oscillators (requirement (vi)). In the context of neuroscience, it means that the stimulation intervention into the living tissue is temporary and smooth (cf. panels showing  $u(t)$  in Figs. 4-7 below).

#### IV. STABILITY ANALYSIS

The complete set of equations for the closed-loop system reads as:

$$\dot{X} = \xi X - \omega_0 Y - X(X^2 + Y^2) - \gamma \cos \beta (\hat{x} \cos \alpha + \hat{y} \sin \alpha) , \quad (11)$$

$$\dot{Y} = \omega_0 X + \xi Y - Y(X^2 + Y^2) - \gamma \sin \beta (\hat{x} \cos \alpha + \hat{y} \sin \alpha) , \quad (12)$$

$$\dot{x}_1 = x_2 , \quad (13)$$

$$\dot{x}_2 = X - \omega_0^2 x_1 - \delta x_2 , \quad (14)$$

$$\dot{x}_3 = \frac{1}{\mu} (x_2 - x_3) , \quad (15)$$

$$\dot{\alpha} = k_\alpha S , \quad (16)$$

$$\dot{\gamma} = k_{\gamma_1} S \cosh^{-1} (k_{\gamma_2} \gamma / \omega_0) , \quad (17)$$

$$\hat{x} = \delta x_2, \quad \hat{y} = \delta \mu \omega_0 x_3 ,$$

$$I = \sqrt{\hat{x}^2 + \hat{y}^2}, \quad S = I [1 + \tanh (k_s (I - h_s))] .$$

As mentioned before, the desired asynchronous state of the population corresponds to the equilibrium point  $(X, Y) = (0, 0)$ . In this section, we will investigate the stability of this point. The stability analysis gives us some insight into selecting appropriate values for the stimulation's parameters.

For simplicity of calculations, using (6), we rewrite the control law (10) as:

$$u = \Upsilon(x_2 + \Pi x_3), \quad (18)$$

where  $\Upsilon = -\gamma\delta \cos \alpha$  and  $\Pi = \mu\omega_0 \tan \alpha$ . For this new representation, we consider the case  $\cos \alpha \neq 0$ . At the points  $\alpha = (2k - 1)\pi/2$ ,  $k = 1, 2, \dots$  the control term is calculated as  $u = \pm\gamma\delta\mu\omega_0 x_3$ .

At the first step of analysis, we study linear stability of the only equilibrium point  $(X, Y, x_1, x_2, x_3) = (0, 0, 0, 0, 0)$  in the absence of adaptation, i.e. for fixed values of  $\alpha$  and  $\gamma$ . For this aim, it is enough to consider linearization of Eqs. (11)-(15). The problem reduces to that of classifying the eigenvalues  $\lambda$  of the state matrix  $\mathcal{A}$  according to their real parts; at stability borders they are purely imaginary  $\lambda = i\Omega$ . This allows one to find stability borders on the planes  $(\Upsilon, \Pi)$  or  $(\alpha, \gamma)$  in a parametric form, as functions of parameter  $\Omega$  (for details see Appendix A). Based on these steps, in Fig. 2 we plot the stability region obtained for the following values of systems' parameters:  $\xi = 0.0048$ ,  $\omega_0 = 2\pi/32.5$ ,  $\delta = 0.3\omega_0$ ,  $\mu = 500$  (we refer to these values in Subsection V A) and six samples of  $\beta$  as representatives of possible values of  $\beta \in [0, 2\pi)$ . It is easy to check that if the point  $(\alpha^*, \gamma^*)$  belongs to the stability borders, then the points  $(\alpha^* \pm 2k\pi, \gamma^*)$  and  $(\alpha^* \pm (2k - 1)\pi, -\gamma^*)$  belong to the stability borders as well.

At the second step of the analysis, we reformulate the linear stability results from Lyapunov theory point of view. Suppose  $\mathfrak{X}$  is the vector of the first five variables in Eqs. (11)-(15), i.e.,  $\mathfrak{X} = (X, Y, x_1, x_2, x_3)^T$ , where the superscript  $T$  denotes the transpose. The linearized system around  $\mathfrak{X} = 0$  can be written as:

$$\dot{\mathfrak{X}} = \mathcal{A}\mathfrak{X}, \quad (19)$$

where the elements of the state matrix  $\mathcal{A}$  are functions of the systems' parameters and variables  $\alpha$  and  $\gamma$ . We have shown that, for each  $\beta$ , there is the stability region (composed of some sub-regions) in the  $\alpha - \gamma$  plane such that if  $\alpha$  and  $\gamma$  are selected in this region, the controlled system Eqs. (11)-(15) is linearly (locally exponentially) stable at  $\mathfrak{X} = 0$ . In other words, independently of the value of  $\beta$ , there is a non-empty region  $\mathcal{N}$  in the positive quadrant, such that for  $(\alpha, \gamma) \in \mathcal{N}$  local exponential stability of the system (19) is guaranteed. As is stated by the converse Lyapunov theorem (<sup>51</sup> Sec. 4.7), there exist a positive definite Lyapunov function  $V_{\mathcal{N}}(\mathfrak{X})$  ( $V_{\mathcal{N}}(\mathfrak{X}) > 0$  and  $V_{\mathcal{N}}(0) = 0$ ) and a region  $\mathcal{N}_S$  ( $\mathcal{N}_S \subset \mathcal{N}$ ) that satisfies the following condition

$$\dot{V}_{\mathcal{N}} = \frac{\partial V_{\mathcal{N}}}{\partial \mathfrak{X}} \dot{\mathfrak{X}} \leq -M(\alpha, \gamma) \|\mathfrak{X}\|^2, \quad \forall (\alpha, \gamma) \in \mathcal{N}_S, \quad (20)$$

for some positive function  $M(\alpha, \gamma)$  which may be the function of other systems' parameters. Here  $\|\cdot\|$  denotes the Euclidean 2-norm. Let  $M_m = \min_{\alpha, \gamma \in \mathcal{N}_s, \beta \in [0, 2\pi)} M(\alpha, \gamma)$ , then Eq. (20) is simplified to:

$$\dot{V}_{\mathcal{N}} \leq -M_m \|\mathfrak{X}\|^2, \quad \forall (\alpha, \gamma) \in \mathcal{N}_S. \quad (21)$$

We refer to (21) later in this section.

At this point we add the dynamics of the adaptive variables  $\alpha$  and  $\gamma$ . Consider the new Lyapunov function  $V = V_{\mathcal{N}} + \frac{1}{2}(\dot{\alpha}^2 + \dot{\gamma}^2)$ .  $V$  is a positive function of its arguments and is equal to zero at  $\mathfrak{X} = 0 = \dot{\alpha} = \dot{\gamma} = 0$ , which according to Eqs. (7)-(9) results in  $I = 0$ . Therefore,  $V$  is a positive definite function and can be a candidate for the Lyapunov function. In the sufficiently small vicinity of  $I = 0$ , the  $S$  function can be approximated by the linear term  $KI$  where  $K = 1 - \tanh(k_s h_s)$ . This approximation leads to the following description for  $\alpha$  and  $\gamma$ :

$$\dot{\alpha} = k_{\alpha} K I, \quad (22)$$

$$\dot{\gamma} = k_{\gamma_1} K I \cosh^{-1}(k_{\gamma_2} / \gamma^* \omega_0), \quad (23)$$

where  $\gamma^*$  is the steady-state value of  $\gamma$ . Now, differentiating the Lyapunov function  $V$  along the trajectories of the augmented system (19), (22) and (23) results in:

$$\begin{aligned} \dot{V} = \dot{V}_{\mathcal{N}} + \dot{\alpha}\ddot{\alpha} + \dot{\gamma}\ddot{\gamma} &= \dot{V}_{\mathcal{N}} + K^2 (k_{\gamma_1}^2 \cosh^{-2}(k_{\gamma_2} \gamma^* / \omega_0) + k_{\alpha}^2) I \dot{I} \\ &\leq \dot{V}_{\mathcal{N}} + K^2 (k_{\gamma_1}^2 + k_{\alpha}^2) I \dot{I}. \end{aligned} \quad (24)$$

Replacing  $I \dot{I} = \delta^2 (x_2 \dot{x}_2 + (\mu \omega_0)^2 x_3 \dot{x}_3)$  in (24) and substituting the dynamics of  $x_2$  and  $x_3$  (Eqs. (14) and (15)), we simplify Eq. (24) to:

$$\dot{V} \leq \dot{V}_{\mathcal{N}} + K^2 (k_{\gamma_1}^2 + k_{\alpha}^2) \mathfrak{X}^T P \mathfrak{X}, \quad (25)$$

where

$$P = \begin{bmatrix} 0 & 0 & 0 & 0.5 & 0 \\ 0 & 0 & 0 & 0 & 0 \\ 0 & 0 & 0 & -0.5\omega_0^2 & 0 \\ 0.5 & 0 & -0.5\omega_0^2 & -\delta & 0.5\mu\omega_0^2 \\ 0 & 0 & 0 & 0.5\mu\omega_0^2 & -\mu\omega_0^2 \end{bmatrix}.$$

We know that  $\mathfrak{X}^T P \mathfrak{X} \leq \lambda_{max}(P) \|\mathfrak{X}\|^2$ , where  $\lambda_{max}(P)$  is the largest eigenvalue of  $P$ . It can be easily checked that  $P$  has two zero eigenvalues and at least one positive eigenvalue. Thus,

$\lambda_{max}(P)$  is non-zero and positive. Based on these properties, Eq. (25) can be rewritten as:

$$\dot{V} \leq \dot{V}_{\mathcal{N}} + \lambda_{max}(P)K^2(k_{\gamma_1}^2 + k_{\alpha}^2) \|\mathfrak{X}\|^2 \quad (26)$$

Using Eq. (21), in the region  $\mathcal{N}_S$  we have:

$$\dot{V} \leq -[M_m - \lambda_{max}(P)K^2(k_{\gamma_1}^2 + k_{\alpha}^2)] \|\mathfrak{X}\|^2, \forall (\alpha, \gamma) \in \mathcal{N}_S \quad (27)$$

Now, if  $\lambda_{max}(P)K^2(k_{\gamma_1}^2 + k_{\alpha}^2) < M_m$ , then  $\dot{V} < 0, \forall (\alpha, \gamma) \in \mathcal{N}_S$ . This means that,  $\|\mathfrak{X}\|$  and, thus, their elements decrease, provided  $(\alpha, \gamma)$  belong to the region  $\mathcal{N}_S$ . Now we have to decide, whether it is possible that during this evolution  $(\alpha, \gamma)$  leave  $\mathcal{N}_S$ . To this end we estimate the total shift of  $(\alpha, \gamma)$ , assuming they enter the region  $\mathcal{N}_S$  with some initial values  $(\alpha_0, \gamma_0)$ . As one can see from (22) and (23), for small  $k_{\alpha}$  and  $k_{\gamma_1}$  these adaptive parameters evolve slowly, so we can separate the time scale of their evolutions from the time scale of the evolution of  $\mathfrak{X}$ ; the latter is determined by  $\lambda_1$ , the closest to the imaginary axis eigenvalue of matrix  $\mathcal{A}$ . In this approximation, the relaxation of the auxiliary oscillating modes is given by  $I = I_0 \exp[\text{Re}(\lambda_1)t]$  (where one can take  $\lambda_1$  in the middle of the region  $\mathcal{N}_S$ ). Substituting this into equations (22) and (23) and then integrating them we get for the shifts of the adaptive parameters

$$\begin{aligned} \Delta\alpha &= k_{\alpha} K I_0 |\text{Re}(\lambda_1)|^{-1}, \\ \Delta\gamma &= k_{\gamma_1} K I_0 |\cosh(k_{\gamma_2}/\gamma^* \omega_0) \text{Re}(\lambda_1)|^{-1}. \end{aligned}$$

Since  $K$  is exponentially small, these shifts are small as well, and thus the adaptive variables  $(\alpha, \gamma)$  remain in the same region  $\mathcal{N}_S$ .

Adaptation parameters  $k_{\alpha}$  and  $k_{\gamma_i}, i = 1, 2$  play the key role in the behavior of the controlled system. They determine the trajectory in the  $(\alpha, \gamma)$  plane. This trajectory always starts from the origin and terminates in one of the stability sub-regions. As it can be seen from Fig. 2, for each  $\beta$ , the stability region consists of periodically arranged sub-regions. Some of them are not accessible by  $\alpha$  and  $\gamma$  because of their increasing dynamics, which keep them in the positive quadrant of the  $\mathbb{R}^2$  space. In Fig. 2 the possible stability sub-regions are shown with the solid lines. For the fixed  $\beta$ , each of these stability sub-regions have the potential to be the terminal point for the adaptive variables. However, the values of the adaptation parameters and also of  $S$  determine, which one will be selected.

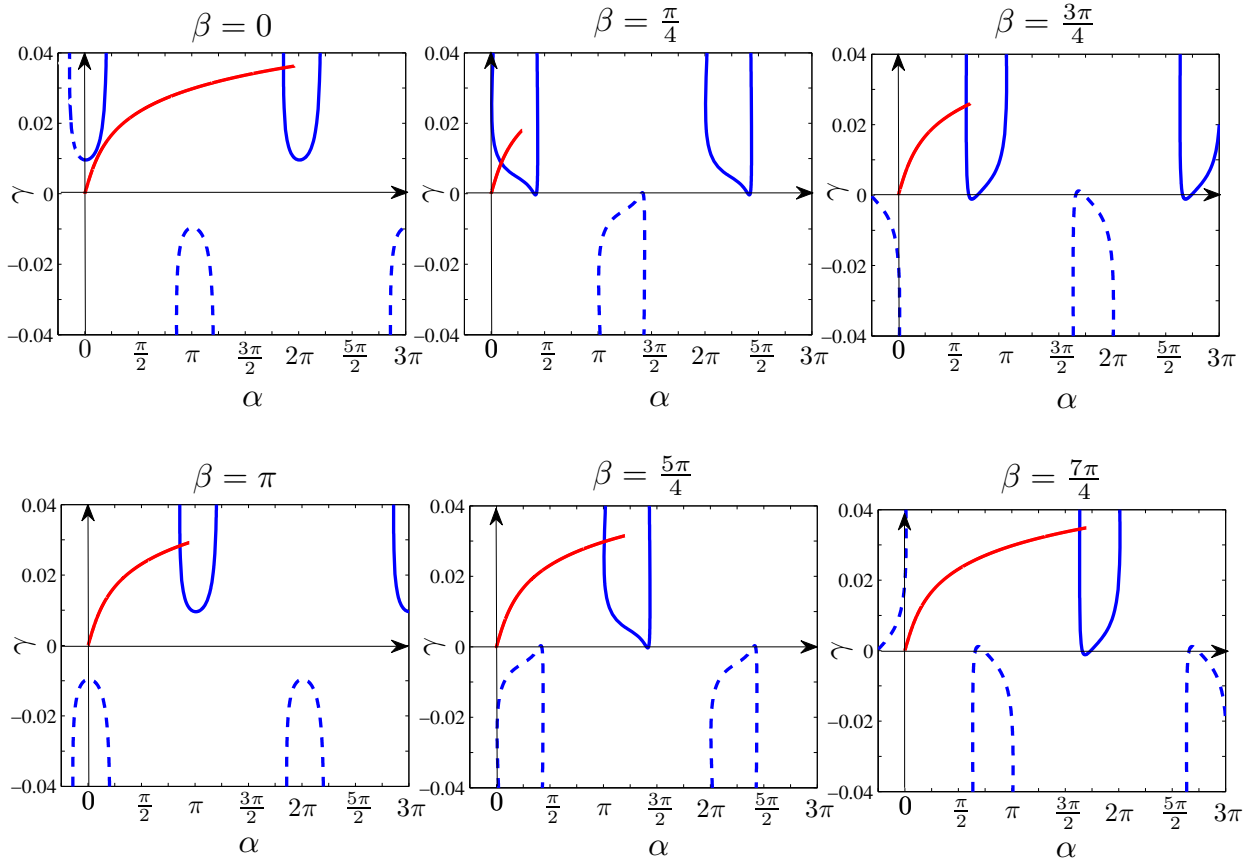


FIG. 2. (Color online) Stability region for the controlled system (11)-(15) consists of closed sub-regions; here they are shown for different values of  $\beta$ . Only areas of the strong stability are shown here. The borders of the stability sub-regions in the positive quadrant are shown by solid lines. (For completeness, we also show by dashed lines the stability borders for negative  $\alpha, \gamma$ .) For each value of  $\beta$ , the trajectory followed by the adaptive variables  $\alpha$  and  $\gamma$  are plotted; eventually, they trap in one of the stability sub-regions.

## V. APPLYING THE ADAPTIVE STIMULATION TO ENSEMBLES OF COUPLED OSCILLATORS

In this section, we apply the proposed stimulation to different ensembles of coupled oscillators. We start by an ensemble of Stuart-Landau oscillators in order to compare the simulation results with the theory. Then, in subsections VB and VC, we perform simulations which reveal the efficiency of the stimulation in desynchronizing ensembles of more complex and realistic oscillators. For better readability, we present the details of parameters

sets in Appendix B.

### A. Stuart-Landau oscillators

A simple Stuart-Landau model reflects the key properties of a self-sustained oscillator. Hence, as the first example, we consider an ensemble of  $N = 1000$  all-to-all coupled and non-identical Stuart-Landau oscillators as:

$$\begin{aligned}\dot{x}_i &= ax_i - \omega_i y_i - x_i(x_i^2 + y_i^2) + CX + u \cos \beta, \\ \dot{y}_i &= \omega_i x_i + ay_i - y_i(x_i^2 + y_i^2) + CY + u \sin \beta,\end{aligned}\tag{28}$$

where  $i = 1, 2, \dots, N$ . Here  $C$  is the strength of the coupling via the mean fields  $X = N^{-1} \sum_i x_i$  and  $Y = N^{-1} \sum_i y_i$  and  $u$  is the control term based on the measured signal  $m = X$ .

Numerical simulations of a non-controlled population show that dynamics of Eqs. (28) with the parameters' values as in Appendix B1 is quite well described by the macroscopic model (2) with  $\xi = 0.0048$  and  $\omega_0 = 2\pi/32.5$ . So, without considering the adaptation mechanism, the borders of the stability region of the controlled system can be analytically approximated by ones plotted in Fig. 2. Now, we want to investigate whether the adaptive mechanism can force  $\alpha$  and  $\gamma$  to trap in one of the stability sub-regions. To this aim, we select  $k_\alpha = 0.003$ ,  $k_{\gamma_1} = 0.0001$  and  $k_{\gamma_2} = 20$ . Then, we simulated the controlled system (28) for several values of  $\beta$ , as shown in sub-panels of Fig. 2. In the  $\alpha - \gamma$  plain, we plot the trajectories tracked by the adaptive variables. As can be seen, for this choice of adaptation parameters all of the  $(\alpha, \gamma)$ -trajectories move toward the nearest stability sub-region (except for  $\beta = 0$ ).

In the next simulation, we make  $\beta$  in (28) time-dependent, as shown in Fig. 3. We plot there also the corresponding evolution of  $\alpha$ . Notice, that in our control scheme parameter  $\alpha$  cannot decrease. One can see that when  $\beta$  increases,  $\alpha$  approximately follows  $\beta$ . When  $\beta$  decreases, first  $\alpha$  avoids to evolve and the controller tries to preserve the obtained asynchronous state based on the previous value of  $\alpha$ . However, larger change of  $\beta$  breaks the controller inertia and forces  $\alpha$  to adapt by increasing by  $\approx 2\pi$  to reach the next stability sub-region.

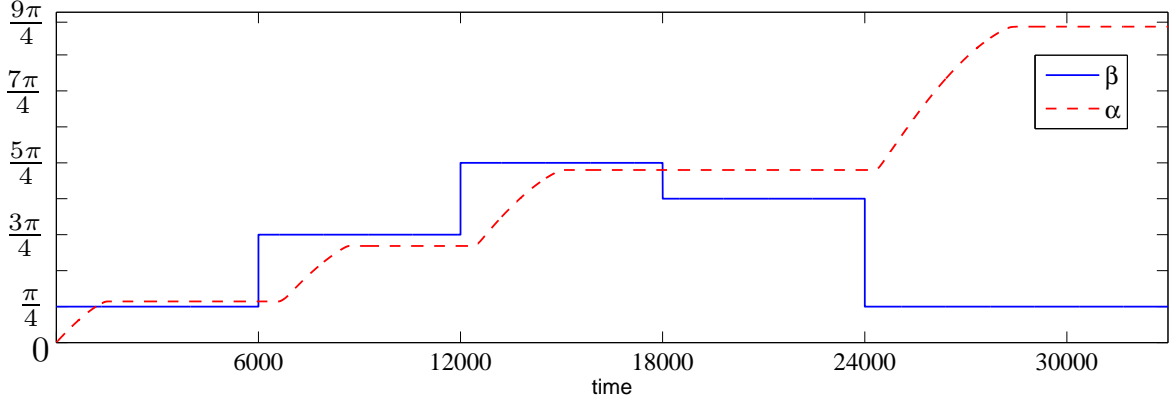


FIG. 3. (Color online) Time course of  $\beta$  in Eqs. (28) (blue solid line) and the corresponding adaptation of  $\alpha$  (red dashed line). For parameters, see Appendix B 1.

## B. Bonhoeffer-van der Pol oscillators

Self-sustained Bonhoeffer-van der Pol oscillator, a system close to the FitzHugh-Nagumo neuron model, oscillates around a non-zero equilibrium points. A population of  $N = 1000$  coupled oscillators under the stimulation  $u$  is described by:

$$\begin{aligned}\dot{x}_i &= x_i - x_i^3/3 - y_i + I_i + CX + u \cos \psi, \\ \dot{y}_i &= 0.1(x_i - 08y_i + 07) + u \sin \psi.\end{aligned}\tag{29}$$

In this example, the impact of the stimulation  $u$  on the oscillators is again distributed between the  $x$  and  $y$  equations according to the value of  $\psi$ . As mentioned in<sup>24</sup>, the parameter  $\psi$  is related but not equal to the phase shift parameter  $\beta$  in Eq. (2). The measured signal  $m = X$  can be considered as contaminated by some intrinsic noise due to the finite ensemble size. Next, it has a non-zero average. Simulation results are depicted in Fig. 4. The stimulation is applied at  $t = 1000$ . Before that, the oscillators are synchronized which is reflected in the large amplitude of the mean field  $X$ . When the stimulation is switched on, it smoothly affects the synchronized oscillators. As a result, the mean field gradually vanishes at the level of the induced noise which in turn results in vanishing stimulation. When the asynchronous state is achieved, the vanishing stimulation maintains it. The evolution of  $\alpha$  and  $\gamma$  is shown in Fig. 4(c) and (d), respectively. Finally, the behaviors of two arbitrary oscillators in the ensemble (Fig. 4(e) and (f)), verify the capability of the stimulation in destroying the synchronous state without destroying individual oscillations.

To show the capability of the proposed stimulation in coping with the case of time-

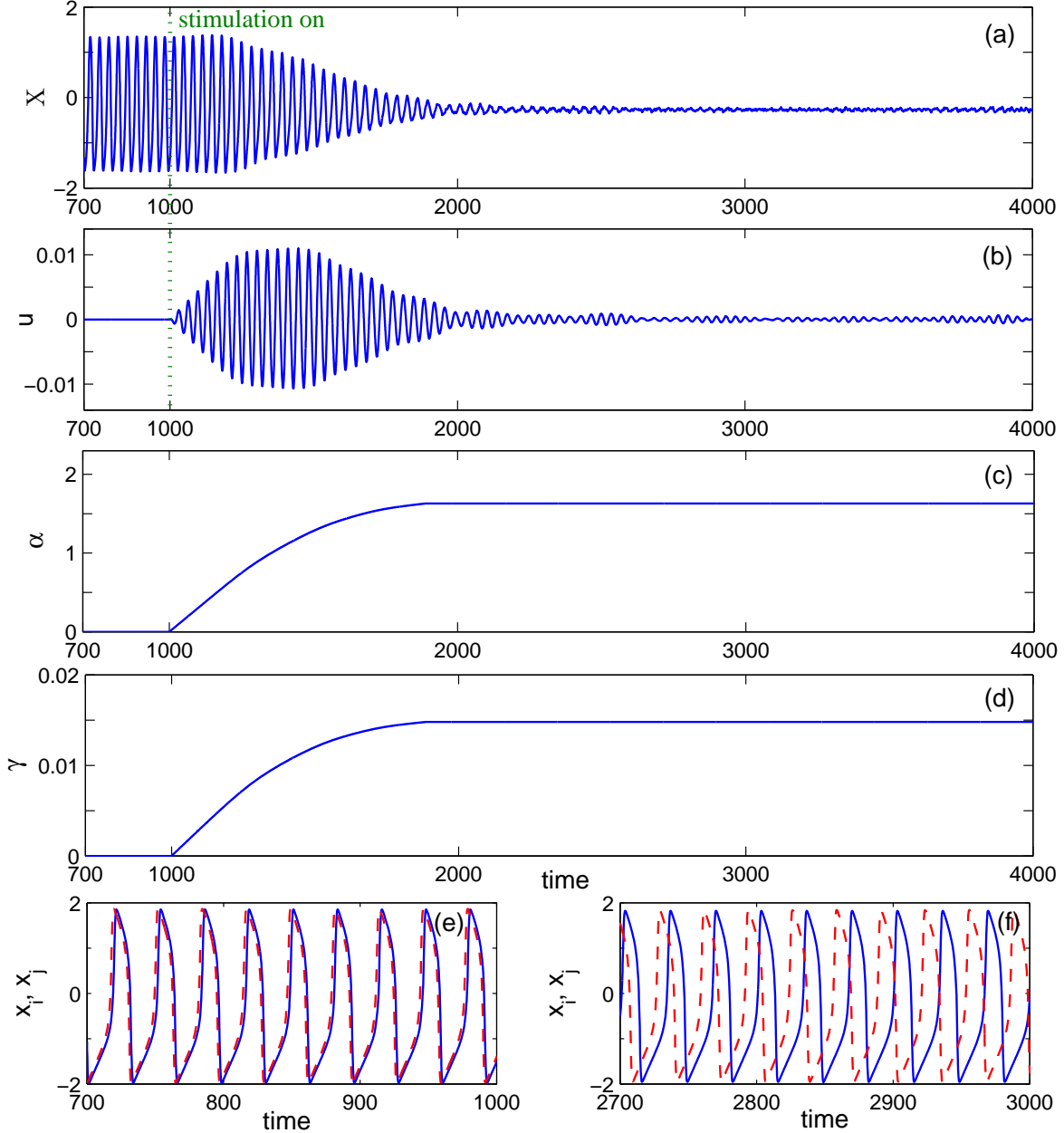


FIG. 4. (Color online) Desynchronization in an ensemble of Bonhoeffer-van der Pol oscillators (29) with  $\psi = \pi/2$ . (a) The mean field  $X$ , (b) the control signal  $u$  and (c),(d) the adaptive variables vs time. (e,f) Synchronous and asynchronous dynamics of two arbitrary chosen oscillators in the ensemble, before and after applying the stimulation, respectively. For parameters see Appendix B 2.

dependent system parameters, in the next simulations (Fig. 5) we vary  $\psi$  as shown in panel (a). The controllers' parameters are as before. As one can see, for  $\psi = 2\pi/3$  the stimulation quenches the mean field. However, as  $\psi$  changes to  $\psi = 4\pi/3$ , the mean field start growing



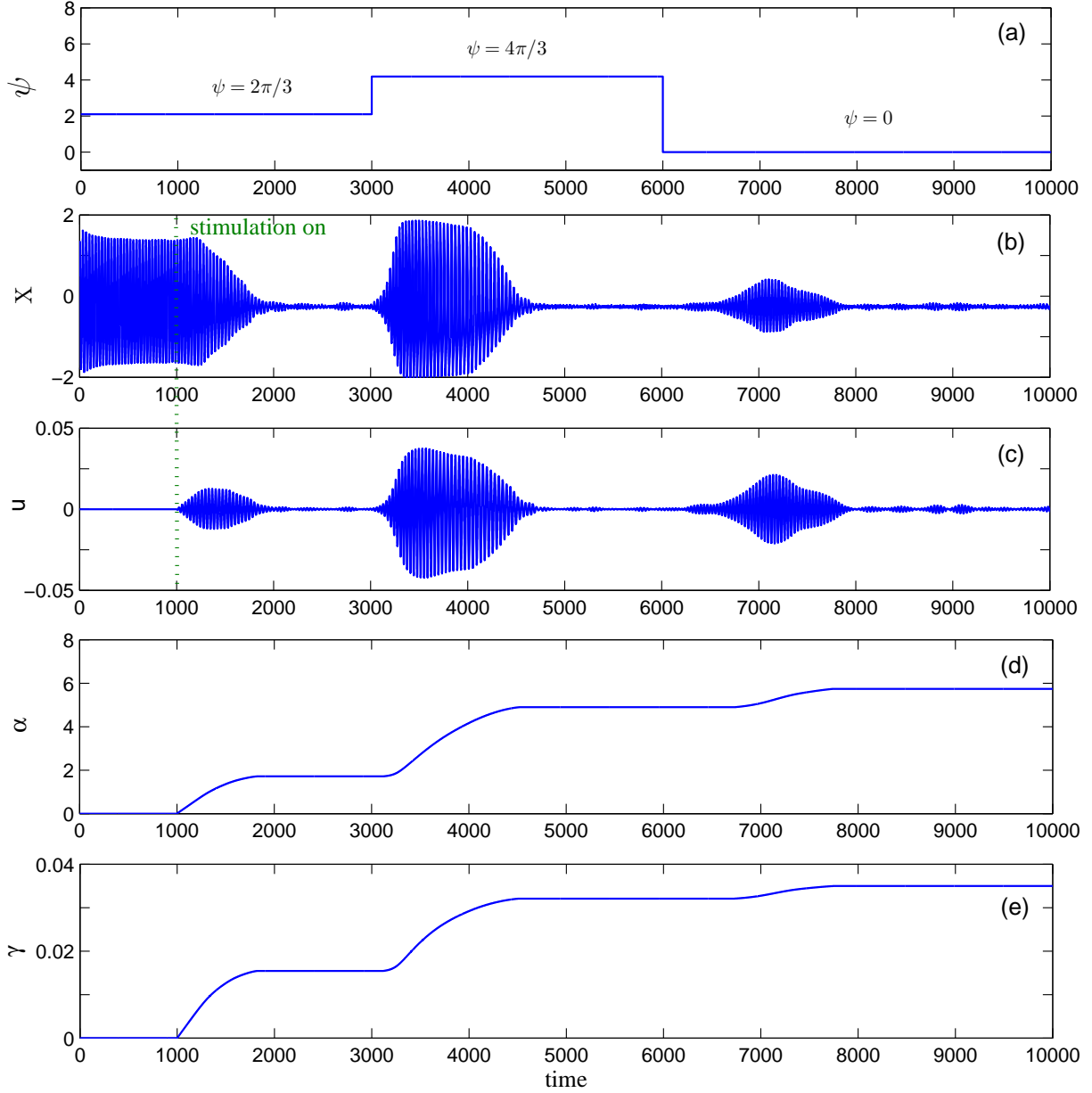


FIG. 5. Suppressing synchrony in an ensemble of Bonhoeffer-van der Pol oscillators in the presence of the time-variant phase shift parameter  $\psi$ . When  $\psi$  changes in time (a), the adaptive variables start to evolve (d) and (e), so that the stimulation (c) adapts itself to the new values of  $\beta$  and stabilizes the mean field (b). Parameters are the same as in Fig. 4.

and the feedback mechanism starts adapting the stimulation to the new situation.  $\alpha$  and  $\gamma$  begin to evolve and finally they settle down to the new values at which the stimulation breaks the synchrony. Depending on the value of  $\psi$ , the new value of the adaptive variables may be found quickly or slowly, which corresponds to fast or slow damping of the mean

field, respectively (compare the damping time for  $\psi = 4\pi/3$  and  $\psi = 0$ ).

Noteworthy, if the already controlled regime needs to be adapted, mostly fast are variations of  $\alpha$ , while variations of  $\gamma$  are slowed down by the denominator in the  $\dot{\gamma}$  equation; with this we minimize the amplitude of achieved feedback control.

### C. Hindmarsh-Rose neurons with synaptic coupling

Since the main purpose of our technique is to suppress neuronal synchrony, in this subsection we analyse a more realistic model. We consider an ensemble of Hindmarsh-Rose neurons and discuss in more detail the measurement of the collective activity and the coupling between the units. The model of  $N$  all-to-all coupled units reads:

$$\begin{aligned} \dot{x}_i &= 3x_i^2 - x_i^3 + y_i - z_i + I_i - \frac{C}{N-1}(x_i + V_c) \sum_{j \neq i}^N \left[ 1 + e^{\left(\frac{x_i - x_0}{\eta}\right)} \right]^{-1} + u, \\ \dot{y}_i &= -5x_i^2 - y_i + 1, \\ \dot{z}_i &= r[\nu(x_i - \chi) - z_i]. \end{aligned} \tag{30}$$

Depending on the value of the parameters, the units show spiking or bursting. Neuronal oscillators in (30) interact via the synaptic connections, described with the inverse exponential term. This type of coupling plays an important role in large networks of neurons where even spatially distant neurons can be linked by long axons.

In our model, the stimulation is described by an additional external current, common for all neurons; it enters equations for  $x$ . Following<sup>24</sup>, we assume, that the measured signal used as an input to the feedback loop is proportional to the derivative of the mean field,  $m = \dot{X} = N^{-1} \sum_i \dot{x}_i$ . The results of applying the adaptive stimulation to  $N = 200$  coupled oscillators (30) in a spiking regime are shown in Fig. 6. Figures 6(a),(b) demonstrate that although the stimulation bases on  $\dot{X}$  instead of  $X$ , it retains its capability in desynchronizing the population. Figures 6(f)-(h) show the behaviors of two arbitrary chosen oscillators before, exactly after, and some time after applying the stimulation, respectively. Comparison of these figures verifies that the stimulation breaks the synchrony without any undesired effect on the individual oscillators. The reason is that the stimulated oscillators are smoothly and gradually affected by the controller.

Next, we consider the case of chaotic bursting, when generation of action potentials alternates with the epochs of quiescence, so that the oscillations can be characterized by

two time scales. The simulation results are shown in Fig. 7.

One important feature in an ensemble of chaotic bursting oscillators is that synchronization occurs on the slower time scale, i.e., different neurons burst nearly at the same time, whereas the spiking within the burst is not synchronous, and therefore is to a large extent averaged out in the mean field. However, due to correlations in spiking, some high frequency fluctuations remain in the mean field. Besides these fluctuations, a low frequency modulation of the mean field is also observed in. In Fig. 7(b), fluctuations and modulation can be seen in the uncontrolled ensemble (i.e.,  $t < 1000$ ). Prior to application of the stimulation, the amplitude of the measured signal  $\dot{X}$  is smaller than it was in the case of spiking neurons (cf. Fig. 7(b) and Fig. 6(b)). This means that  $I$  and consequently  $S$  are smaller as well. If we select the same adaptive parameters as for the spiking neurons, the adaptive variables  $\alpha$  and  $\gamma$  vary very slowly and desynchronization takes quite a large time. Therefore, we select larger values for the adaptation parameters  $k_\alpha$  and  $k_{\gamma_1}$  to speed up the dynamics of  $\alpha$  and  $\gamma$ . In addition,  $h_s$  is taken smaller to be in harmony with the switch input  $I$ . When the stimulation is switched on, it suppresses the observed periodic components in  $X$ . Figure 7(f) reveals that impact of the stimulation is smooth and two arbitrary chosen neurons gradually desynchronize.

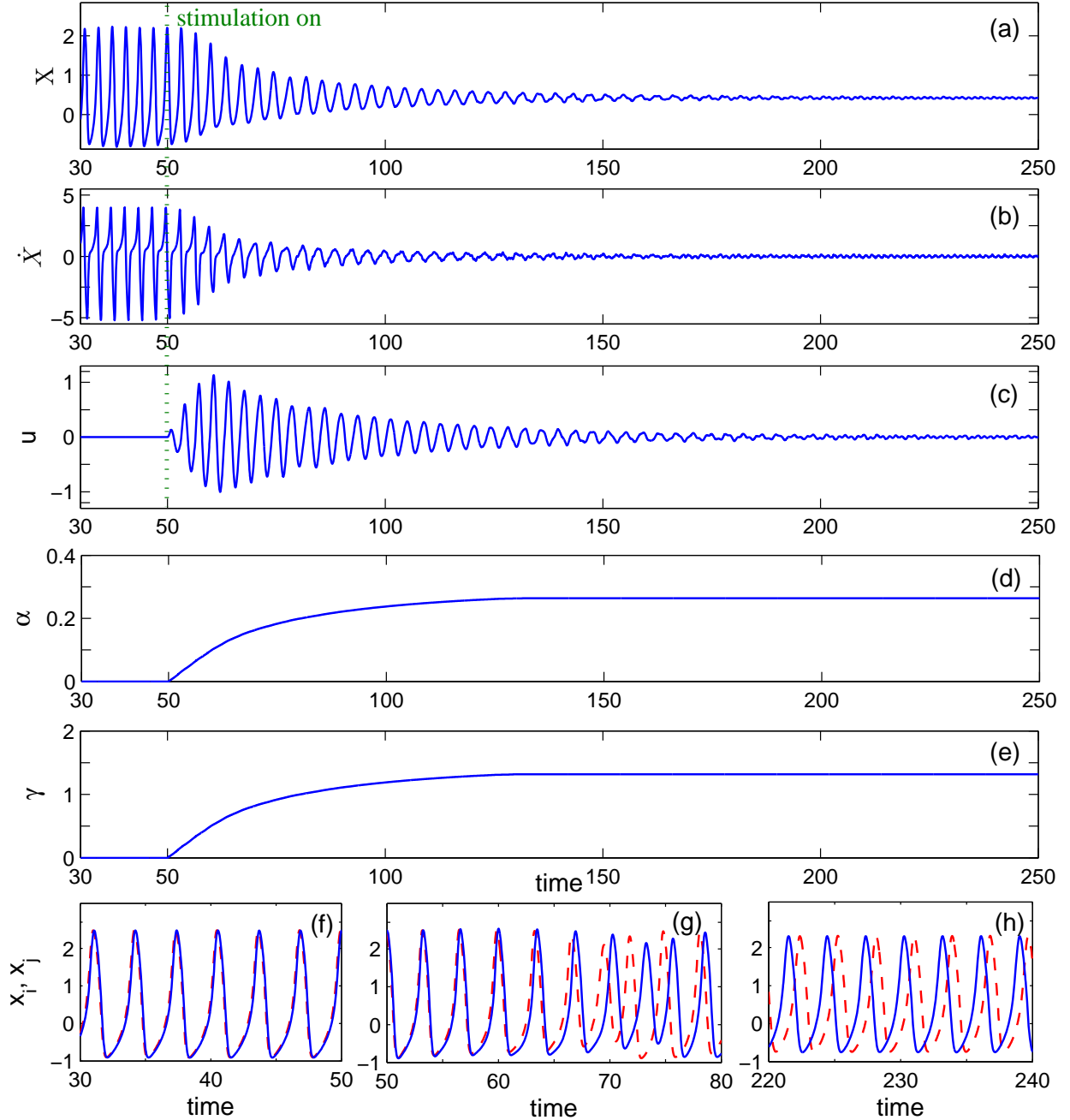


FIG. 6. (Color online) Suppression of synchrony in an ensemble of synaptically coupled spiking Hindmarsh-Rose neurons. (a)-(c) The mean field, its derivative (which is used as a measured signal) and the control signal  $u$ , respectively. Time courses of the adaptive variables (d) and (e). The behavior of two arbitrary chosen oscillators in the ensemble, before (f), exactly after (g), and some time after applying the stimulation (h). For parameters, see Appendix B 3.

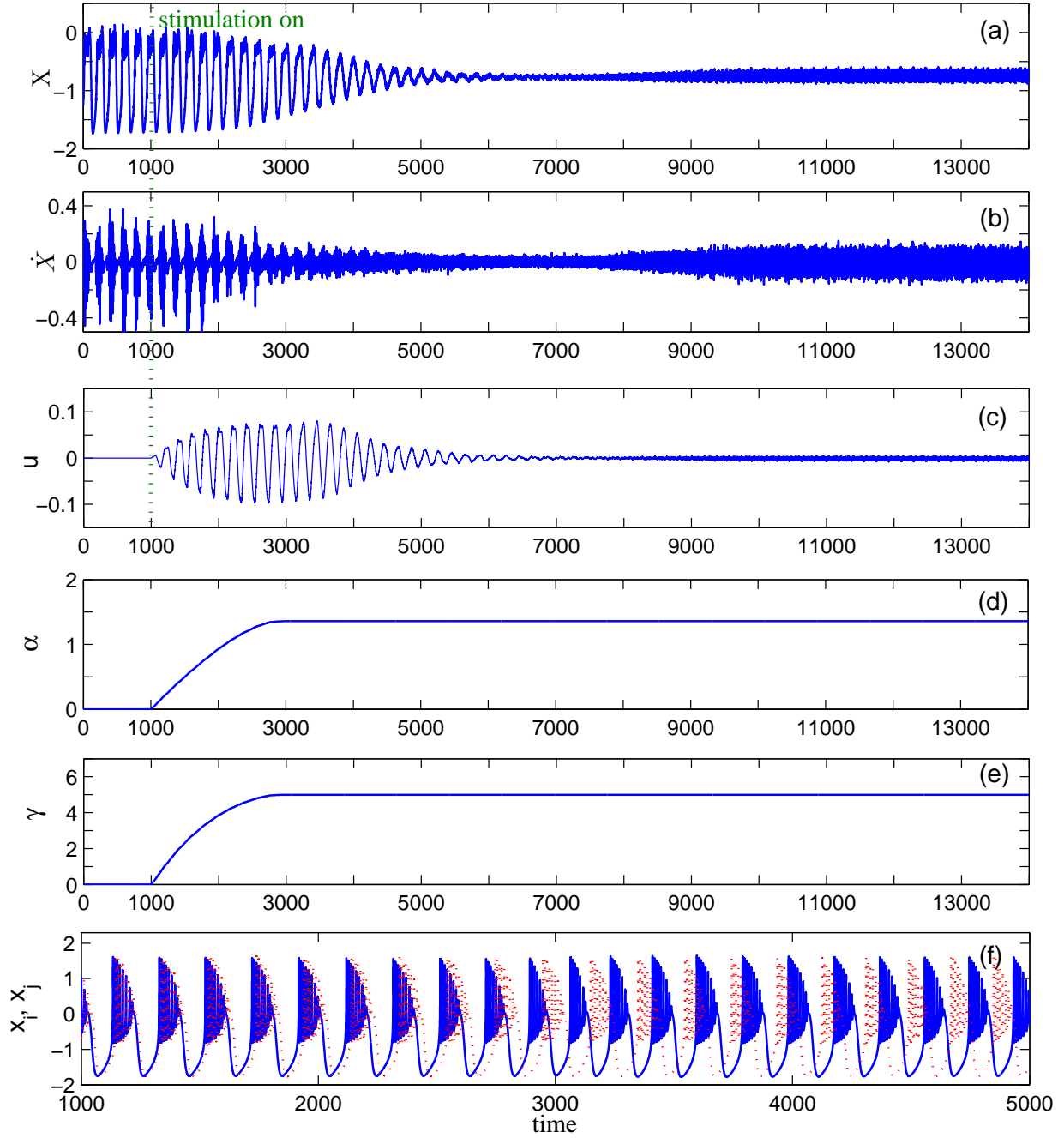


FIG. 7. (Color online) Suppression of synchrony in an ensemble of synaptically coupled bursting Hindmarsh-Rose neurons. (a)-(c) The mean field, its derivative (which is used as a measured signal) and the control signal  $u$ , respectively. (d) and (e) Time courses of the adaptive variables. (f) Transition from synchrony to asynchrony illustrated with two arbitrary chosen elements of the ensemble. For parameters, see Appendix B 4.

## VI. CONCLUSION

In this paper we have suggested a simple adaptive method for achieving desynchronization in populations of oscillators via a vanishing feedback stimulation. The adaptation is required because a macroscopic description of a globally coupled ensemble in terms of the model equation (2) requires knowledge of three parameters. One of them, the oscillation frequency, can be easily determined from the data, while the instability of the equilibrium  $\xi$  and the phase parameter  $\beta$  cannot. Therefore, two parameters, characterizing the feedback loop, namely its strength and the phase shift, cannot be determined *a priori* and should be either found by trial or by an automated adaptation algorithm.

We have shown that, introducing an adaptive adjustment of two parameters in the feedback loop, it is possible to overcome the uncertainty in the dynamics of the mean field, varying the additional phase parameter and gradually increasing the amplification of the feedback loop in such a way, that a robust asynchronous state is achieved and maintained by a vanishingly small stimulation. Moreover, sudden or smooth variations of this phase shift are successfully followed by the adaptation, so that after some transients asynchronous state re-establishes.

Along with the linear analysis of the scheme, we demonstrated its feasibility on a range of models of coupled oscillators. The most nontrivial of them are populations of spiking and bursting neurons, described by the Hindmarsh-Rose model. We also discussed possible restrictions on the adaptation parameters, although a more detailed consideration is needed in each case where the characteristic time scales and degree of non-stationarity of the underlying system are available.

Our research was motivated by recent studies related to neuroscience. However, the formulation of the control problem is quite general and is applicable to other situations where desynchronization of a system with unknown parameters is desirable.

## ACKNOWLEDGMENTS

We thank A. Pogromsky for helpful discussions. G. M. acknowledges financial support from the German Academic Exchange Service (DAAD).

## Appendix A: Computing the stability domain

The characteristic equation of the first five equations in (11) reads:

$$\begin{aligned}
& \lambda^5 \mu + \lambda^4 (1 + \delta \mu - 2\xi \mu) + \lambda^3 (\xi^2 \mu - \Upsilon \mu \cos \beta + 2\omega_0^2 \mu \\
& - 2\xi \delta \mu + \delta - 2\xi) + \lambda^2 (\omega_0^2 \delta \mu - \Upsilon \cos \beta - \Upsilon \Pi \cos \beta \\
& - 2\xi \omega_0^2 \mu - 2\xi \delta + \Upsilon \xi \mu \cos \beta + \xi^2 \delta \mu + \Upsilon \omega_0 \mu \sin \beta + 2\omega_0^2 \\
& + \xi^2) + \lambda (\Upsilon \omega_0 \sin \beta + \Upsilon \xi \cos \beta + \Upsilon \Pi \omega_0 \sin \beta + \xi^2 \omega_0^2 \mu \\
& + \omega_0^4 \mu + \omega_0^2 \delta + \xi^2 \delta - 2\xi \omega_0^2 + \Upsilon \Pi \xi \cos \beta) + \xi^2 \omega_0^2 + \omega_0^4 \\
& = 0
\end{aligned} \tag{A1}$$

The stability domain in the  $\Pi - \Upsilon$  plane or, equivalently, in the  $\alpha - \gamma$  plane corresponds to the condition  $\text{Re}(\lambda) < 0$ . Thus,  $\text{Re}(\lambda) = 0$  gives the border of the stability region. Therefore, taking  $\lambda = i\Omega$  in the (A1) and separating real and imaginary parts, we obtain:

$$\begin{aligned}
& \Omega^4 (1 + \delta \mu - 2\xi \mu) + \Omega^2 [\Upsilon \cos \beta (1 - \xi \mu + \Pi) \\
& - \Upsilon \omega_0 \mu \sin \beta + 2\xi \omega_0^2 \mu + 2\xi \delta - \omega_0^2 \delta \mu - \xi^2 \delta \mu - 2\omega_0^2 \\
& - \xi^2] + \xi^2 \omega_0^2 + \omega_0^4 = 0,
\end{aligned} \tag{A2a}$$

$$\begin{aligned}
& \Omega \{ \Omega^4 \mu + \Omega^2 [\mu (\Upsilon \cos \beta - \xi^2 - 2\omega_0^2 + 2\xi \delta) - \delta + 2\xi] \\
& + \Upsilon (1 + \Pi) (\omega_0 \sin \beta + \xi \cos \beta) + \omega_0^2 (\xi^2 \mu + \delta - 2\xi) \\
& + \omega_0^4 \mu + \xi^2 \delta \} = 0.
\end{aligned} \tag{A2b}$$

Since  $\Omega = 0$  provides no solution, we divide (A2b) by  $\Omega \neq 0$ . Now, parameters  $\Upsilon$  and  $\Pi$  can be extracted by solving (A2a) and (A2b) as:

$$\Pi = T_1/T_2, \quad \Upsilon = T_3/T_4, \tag{A3}$$

where

$$\begin{aligned}
T_1 &= \omega_0 \sin \beta [\Omega^6 \mu^2 + \Omega^4 (1 - 2\omega_0^2 \mu^2 + 2\mu^2 \xi \delta - \mu^2 \xi^2) \\
&\quad + \Omega^2 (\omega_0^2 \mu^2 \xi^2 - 2\omega_0^2 + \omega_0^4 \mu^2 + 2\xi \delta - \xi^2) + \xi^2 \omega_0^2 + \omega_0^4] \\
&\quad + \cos \beta [\Omega^6 (\delta \mu^2 - \xi \mu^2) + \Omega^4 (\delta - \xi - \xi^3 \mu^2 + \xi^2 \mu^2 \delta \\
&\quad - \omega_0^2 \delta \mu^2) + \Omega^2 (\xi^2 \delta - \omega_0^2 \delta - \xi^3 + \xi \mu^2 \omega_0^4 + \xi^3 \mu^2 \omega_0^2) \\
&\quad + \xi^3 \omega_0^2 + \omega_0^4 \xi] , \\
T_2 &= \omega_0 \sin \beta [\Omega^4 (2\xi \mu - \delta \mu - 1) + \Omega^2 (\xi^2 \delta \mu - 2\xi \omega_0^2 \mu - 2\xi \delta \\
&\quad + \xi^2 + \omega_0^2 + \omega_0^2 \delta \mu) - \xi^2 \omega_0^2 - \omega_0^4] + \cos \beta [\Omega^6 \mu + \Omega^4 (\delta \xi \mu \\
&\quad + \xi^2 \mu - 2\omega_0^2 \mu + \xi - \delta) + \Omega^2 (\omega_0^4 \mu - \xi^2 \omega_0^2 \mu + \omega_0^2 \xi \mu \delta \\
&\quad + \xi^3 \delta \mu - \xi^2 \delta + \omega_0^2 \delta + \xi^3) - \xi^3 \omega_0^2 - \omega_0^4 \xi] , \\
T_3 &= \cos \beta [-\Omega^6 \mu + \Omega^4 (2\omega_0^2 \mu - \xi^2 \mu - \mu \xi \delta + \delta - \xi) \\
&\quad + \Omega^2 (\omega_0^2 \xi^2 \mu - \xi^3 - \omega_0^4 \mu - \xi^3 \delta \mu - \omega_0^2 \mu \xi \delta + \xi^2 \delta - \omega_0^2 \delta) \\
&\quad + \xi^3 \omega_0^2 + \omega_0^4 \xi] + \omega_0 \sin \beta [\Omega^4 (1 - 2\mu \xi + \delta \mu) + \Omega^2 (2\xi \delta \\
&\quad + 2\xi \omega_0^2 \mu - \omega_0^2 \delta \mu - \xi^2 \delta \mu - \xi^2 - 2\omega_0^2) + \omega_0^4 + \xi^2 \omega_0^2] , \\
T_4 &= \mu \Omega^2 [\xi \omega_0 \sin 2\beta + \omega_0^2 + \cos^2 \beta (\Omega^2 + \xi^2 - \omega_0^2)] .
\end{aligned} \tag{A4}$$

Now, for each value of  $\Omega$ , using (18), we compute:

$$\alpha = \arctan (T_1/T_2\mu\omega_0), \quad \gamma = -T_3/T_4\delta \cos \alpha \tag{A5}$$

## Appendix B: Parameters of oscillators ensembles

### 1. Stuart-Landau oscillators

For the Stuart-Landau oscillators (28),  $a = 0.01$  and  $\omega_i$  are selected from a Gaussian distribution with the mean value  $w_0 = 2\pi/32.5$  and rms value 0.001;  $C = 0.008$ . With these values of parameters, the mean field's dynamics can be approximated by Eq.(1) with  $\xi = 0.0048$  and  $\omega_0 = 2\pi/32.5$ . For the bandpass filter and the integrator we select  $\delta = 0.3\omega_0$  and  $\mu = 500$ . These values are exactly the same as the ones used for the simulations shown in Fig. 2. The switch and the adaptation parameters are selected as  $h_s = 0.05$ ,  $k_s = 200$  and  $k_\alpha = 0.003$ ,  $k_{\gamma_1} = 0.0001$ ,  $k_{\gamma_2} = 20$ , respectively.



## 2. Bonhoeffer-Van der Pol oscillators

In (29),  $I_i$  are selected from a Gaussian distribution with the mean value 0.6 and rms value 0.1. When  $u = 0$  and  $C < 0.018$  the mean field  $X$  shows small irregular fluctuations around  $X_0 = -0.26$ . These fluctuations are due to the finite size of the population. Since the equilibrium point of the individual oscillators is not at zero, the mean field has a constant term. For  $C > 0.018$  the population synchronizes which leads to large oscillation of  $X$ . For simulation we take  $N = 1000$  and the following parameters' values:  $C = 0.03$ ,  $\omega_0 = 2\pi/32.5$ ,  $\delta = 0.3\omega_0$ ,  $h_s = 0.2$ ,  $k_s = 500$ ,  $k_\alpha = 0.001$ ,  $k_{\gamma_1} = 10^{-5}$ , and  $k_{\gamma_2} = 10$ .

## 3. Spiking Hindmarsh-Rose neurons

In the Hindmarsh-Rose neuron model (30), we set the parameters' values as:  $r = 0.006$ ,  $\nu = 1$ , and  $\chi = -1.56$ . The coupling strength is  $C = 0.4$  which results in synchronous oscillations in the absence of the stimulation  $u$ . Other parameters of synapses are  $\eta = 0.01$ ,  $x_0 = 0.85$ , and inverse potential  $V_c = 1.4$ . The external current  $I_i$  is taken as  $I_i = 6 + \sigma$ , where  $\sigma$  is Gaussian distributed with zero mean and 0.1 rms value.

Without the stimulation, the synchronized ensemble shows oscillations with the average frequency  $\omega_0 = 2\pi/3.2$ . Again, the parameters of the filter and the integrator are  $\delta = 0.3\omega_0$  and  $\mu = 500$ . Finally, the parameters' values of the adaptive stimulation are:  $h_s = 0.15$ ,  $k_s = 200$ ,  $k_\alpha = 0.002$ ,  $k_{\gamma_1} = 0.01$ , and  $k_{\gamma_2} = 0.01$ .

## 4. Bursting Hindmarsh-Rose neurons

The chaotic bursting oscillation in (30) are obtained by taking  $\nu = 4$ ,  $\chi = -1.6$ , and  $I_i = 3.2$ . Parameters of the coupling are kept as before. The coupling strength  $C = 0.2$ . The average frequency of the mean field is  $\omega_0 = 2\pi/176$ . The stimulation's parameters are as follows: switch parameters  $h_s = 0.01$ ,  $k_s = 500$ , adaptation parameters  $k_\alpha = 0.02$ ,  $k_{\gamma_1} = 0.1$ , and  $k_{\gamma_2} = 0.01$ .

## REFERENCES

- <sup>1</sup>A. S. Pikovsky, M. G. Rosenblum, and J. Kurths, *Synchronization: A Universal Concept in Nonlinear Sciences* (Cambridge University Press, New York, 2001).
- <sup>2</sup>E. Mosekilde, D. Postnov, and Y. Maistrenko, *Chaotic Synchronization: Applications to Living Systems* (World Scientific, Singapore, 2002).
- <sup>3</sup>S. H. Strogatz, *Sync: The Emerging Science of Spontaneous Order* (Hyperion Books, New York, 2003).
- <sup>4</sup>A. Balanov, N. Janson, D. Postnov, and O. Sosnovtseva, *Synchronization: From Simple to Complex* (Springer, New York, 2009).
- <sup>5</sup>D. Cumin and C. P. Unsworth, “Generalising the Kuramoto model for the study of neuronal synchronization in the brain,” *Physica D* **226**, 181–196 (Feb. 2007).
- <sup>6</sup>P. A. Tass, *Phase Resetting in Medicine and Biology. Stochastic Modelling and Data Analysis* (Springer-Verlag, Berlin, 1999).
- <sup>7</sup>*Epilepsy as a Dynamic Disease*, edited by J. Milton and P. Jung (Springer, Berlin, 2003).
- <sup>8</sup>G. Buzsáki and A. Draguhn, “Neuronal oscillations in cortical networks,” *Science* **304**, 1926–1929 (2004).
- <sup>9</sup>C.A.S. Batista, S.R. Lopes, R. L. Viana, and A. M. Batista, “Delayed feedback control of bursting synchronization in a scale-free neuronal network,” *Neural Networks* **23**, 114–124 (Jan. 2010).
- <sup>10</sup>C. Park, R. M. Worth, and L. L. Rubchinsky, “Neural dynamics in parkinsonian brain: The boundary between synchronized and nonsynchronized dynamics,” *Phys. Rev. E* **83**, 042901 (Oct. 2011).
- <sup>11</sup>S. A. Chkhenkeli, *Bull. of Georgian Academy of Sciences* **90**, 406–411 (1978).
- <sup>12</sup>S. A. Chkhenkeli, “Direct deep brain stimulation: First steps towards the feedback control of seizures,” in *Epilepsy as a Dynamic Disease*, edited by J. Milton and P. Jung (Springer, Berlin, 2003) pp. 249–261.
- <sup>13</sup>A. L. Benabid, P. Pollak, C. Gervason, D. Hoffmann, D M. Gao, M. Hommel, J. E. Perret, and J. de Rougemont, “Long-term suppression of tremor by chronic stimulation of the ventral intermediate thalamic nucleus,” *Lancet*. **337**, 403–406 (feb 1991).
- <sup>14</sup>M. L. Kringelbach, N. Jenkinson, S. L. F. Owen, and T. Z. Aziz, “Translational principles of deep brain stimulation,” *Nat Rev Neurosci* **8**, 623–635 (2007).

- <sup>15</sup>J. M. Bronstein, M. Tagliati, R.L. Alterman, A.M. Lozano, J. Volkmann, A. Stefani, F.B. Horak, M.S. Okun, K.D. Foote, P. Krack, R. Pahwa, J.M. Henderson, M.I. Hariz, R.A. Bakay, A. Rezai, W.I. Marks, Jr, E. Moro, J.L. Vitek, F.M. Weaver, R.E. Gross, and M.R. DeLong, “Deep brain stimulation for parkinson disease: an expert consensus and review of key issues,” *Arch Neurol.* **68**, 165 (2011).
- <sup>16</sup>C. Hammond, R. Ammari, B. Bioulac, and L. Garcia, “Latest view on the mechanism of action of deep brain stimulation,” *Mov. Disord.* **23**, 2111–2121 (nov 2008).
- <sup>17</sup>B. Rosin, M. Slovik, R. Mitelman, M. Rivlin-Etzion, S. N. Haber, Z. Israel, E. Vaadia, and H. Bergman, “Closed-loop deep brain stimulation is superior in ameliorating parkinsonism,” *Neuron* **72**, 370–384 (Oct. 2011).
- <sup>18</sup>A. Berényi, M. Belluscio, D. Mao, and G. Buzsáki, “Closed-loop control of epilepsy by transcranial electrical stimulation,” *Science* **337**, 735–737 (Aug. 2012).
- <sup>19</sup>P. A. Tass, “A model of desynchronizing deep brain stimulation with a demand-controlled coordinated reset of neural subpopulations,” *Biol. Cybern.* **89**, 81–88 (Aug. 2003).
- <sup>20</sup>B. Lysyansky, O. V. Popovych, and P. A. Tass, “Desynchronizing anti-resonance effect of  $m : n$  on-off coordinated reset stimulation,” *J. Neural Eng.* **8**, 036019 (Jun. 2011).
- <sup>21</sup>M. G. Rosenblum and A. S. Pikovsky, “Controlling synchronization in an ensemble of globally coupled oscillators,” *Phys. Rev. Lett.* **92**, 114102 (Mar. 2004).
- <sup>22</sup>M. G. Rosenblum and A. S. Pikovsky, “Delayed feedback control of collective synchrony: an approach to suppression of pathological brain rhythms,” *Phys. Rev. E* **70**, 041904 (2004).
- <sup>23</sup>O. V. Popovych, C. Hauptmann, and P. A. Tass, “Control of neuronal synchrony by nonlinear delayed feedback,” *Biol. Cybern.* **95**, 69–85 (Jul. 2006).
- <sup>24</sup>N. Tukhlina, M. G. Rosenblum, A. S. Pikovsky, and J. Kurths, “Feedback suppression of neural synchrony by vanishing stimulation,” *Phys. Rev. E* **75**, 011918 (2007).
- <sup>25</sup>K. Pyragas, O. V. Popovych, and P. A. Tass, “Controlling synchrony in oscillatory networks with a separate stimulation-registration setup,” *Europhys. Lett.* **80**, 40002 (2007).
- <sup>26</sup>O. V. Popovych, C. Hauptmann, and P. A. Tass, “Impact of nonlinear delayed feedback on synchronized oscillators,” *J. Biol. Phys.* **34**, 367–379 (Nov. 2008).
- <sup>27</sup>Y. Kobayashi and H. Kori, “Design principle of multi-cluster and desynchronized states in oscillatory media via nonlinear global feedback,” *New J. Phys.* **11**, 033018 (Mar. 2009).

- <sup>28</sup>M. Luo, Y. Wu, and J. Peng, “Washout filter aided mean field feedback desynchronization in an ensemble of globally coupled neural oscillators,” *Biol. Cybern.* **101**, 241–246 (Sep. 2009).
- <sup>29</sup>O. V. Popovych and P. A. Tass, “Synchronization control of interacting oscillatory ensembles by mixed nonlinear delayed feedback,” *Phys. Rev. E* **82**, 026204 (Aug. 2010).
- <sup>30</sup>M. Luo and J. Xu, “Suppression of collective synchronization in a system of neural groups with washout-filter-aided feedback,” *Neural Networks* **24**, 538–543 (Aug. 2011).
- <sup>31</sup>A. Franci, A. Chaillet, and W. Pasillas-Lépine, “Existence and robustness of phase-locking in coupled Kuramoto oscillators under mean-field feedback,” *Automatica* **47**, 1193–1202 (Jun. 2011).
- <sup>32</sup>A. Franci, A. Chaillet, E. Panteley, and F. Lamnabhi-Lagarrigue, “Desynchronization and inhibition of Kuramoto oscillators by scalar mean-field feedback,” *Math. Control Signals Syst.* **24**, 169–217 (Apr. 2012).
- <sup>33</sup>C. Hauptmann, O. V. Popovych, and P. A. Tass, “Demand-controlled desynchronization of oscillatory networks by means of a multisite delayed feedback stimulation,” *Comp. Visual. Sci.* **10**, 71–78 (Jun. 2007).
- <sup>34</sup>O. E. Omel’chenko, C. Hauptmann, Yu. L. Maistrenko, and P. A. Tass, “Collective dynamics of globally coupled phase oscillators under multisite delayed feedback stimulation,” *Physica D* **237**, 365–384 (Mar. 2008).
- <sup>35</sup>Y. Guo and J. E. Rubin, “Multi-site stimulation of subthalamic nucleus diminishes thalamocortical relay errors in a biophysical network model,” *Neural Networks* **24**, 602–616 (Aug. 2011).
- <sup>36</sup>M. G. Rosenblum, N. Tukhlina, A. S. Pikovsky, and L. Cimponeriu, “Delayed feedback suppression of collective rhythmic activity in a neuronal ensemble,” *Int. J. of Bifurcation and Chaos* **16**, 1989–1999 (2006).
- <sup>37</sup>N. Tukhlina and M. G. Rosenblum, “Feedback suppression of neural synchrony in two interacting populations by vanishing stimulation,” *J. Biol. Phys.* **34**, 301–314 (Jul. 2008).
- <sup>38</sup>E. Ott and Th. M. Antonsen, “Low dimensional behavior of large systems of globally coupled oscillators,” *CHAOS* **18**, 037113 (2008).
- <sup>39</sup>E. Ott and Th. M. Antonsen, “Long time evolution of phase oscillator systems,” *CHAOS* **19**, 023117 (2009).

- <sup>40</sup>S. Schikora, P. Hövel, H.-J. Wünsche, E. Schöll, and F. Henneberger, “All-optical noninvasive control of unstable steady states in a semiconductor laser,” *Phys. Rev. Lett.* **97**, 213902 (Nov 2006), <http://link.aps.org/doi/10.1103/PhysRevLett.97.213902>.
- <sup>41</sup>J. Kaloust and Z. Qu, “Robust control design for nonlinear uncertain systems with an unknown time-varying control direction,” *IEEE Trans. Autom. Cntr.* **42**, 393–399 (Mar. 1997).
- <sup>42</sup>J.X. Xu and R. Yan, “Iterative learning control design without a priori knowledge of the control direction,” *Automatica* **40**, 1803–1809 (Oct. 2004).
- <sup>43</sup>J. Kaloust and Z. Qu, “Continuous robust control design for nonlinear uncertain systems without a priori knowledge of control direction,” *IEEE Trans. Autom. Cntr.* **40**, 276–282 (Feb. 1995).
- <sup>44</sup>S. S. Ge, C. Yang, and T. H. Lee, “Adaptive robust control of a class of nonlinear strict-feedback discrete-time systems with unknown control directions,” *Syst. Control Lett.* **57**, 888–895 (Nov. 2008).
- <sup>45</sup>L. Liu and J. Huang, “Global robust output regulation of lower triangular systems with unknown control direction,” *Automatica* **44**, 1278–1284 (May 2008).
- <sup>46</sup>Y. Wen and X. Ren, “Neural networks-based adaptive control for nonlinear time-varying delays systems with unknown control direction,” *IEEE Trans. Neural Networks* **22**, 1599–1612 (Oct. 2011).
- <sup>47</sup>G. Bartolini, A. Pisano, and E. Usai, “On the second-order sliding mode control of nonlinear systems with uncertain control direction,” *Automatica* **45**, 2982–2985 (Dec. 2009).
- <sup>48</sup>A second order system in the strict feedback form is represented as  $\dot{x}_1 = f_1(x_1) + g_1x_2$ ,  $\dot{x}_2 = f_2(x_1, x_2) + g_2u$ , where  $g_{1,2}$  are unknown parameters. A  $(2 + m)^{th}$  order system in the normal form is represented as  $\dot{x}_1 = x_2$ ,  $\dot{x}_2 = f(x_1, x_2, y) + gu$ ,  $\dot{y} = q(x_1, x_2, y)$ , where  $y \in \mathbb{R}^m$  is the vector of additional states (which describe internal dynamics of the feedback loop; see Ref.<sup>51</sup> for more details).
- <sup>49</sup>T. R. Oliveira, A. J. Peixoto, and L. Hsu, “Sliding mode control of uncertain multivariable nonlinear systems with unknown control direction via switching and monitoring function,” *IEEE Trans. Autom. Cntr.* **55**, 1028–1034 (2010).
- <sup>50</sup>A. Pikovsky and S. Ruffo, “Finite-size effects in a population of interacting oscillators,” *Phys. Rev. E.* **59**, 1633 (1999).
- <sup>51</sup>H. K. Khalil, *Nonlinear Control Systems* (Prentic Hall, New Jersey, 2002).